applied sciences

MDPI

Article

Characteristics of TiN Thin Films Deposited by Substrate Temperature Variables Using Scanning Acoustic Microscopy

Dongchan Kang [1], Young Sung Kim [2], Jeong Nyeon Kim [3] and Ik Keun Park [4,*]

[1] Graduate School of Nano IT Design Fusion, Seoul National University of Science and Technology, 232 Gongneung-ro, Nowon-gu, Seoul 01811, Korea; dongchan@seoultech.ac.kr
[2] SeoulTech NDT Research Center (SNDT), Seoul National University of Science and Technology, 232 Gongneung-ro, Nowon-gu, Seoul 01811, Korea; youngsk@seoultech.ac.kr
[3] Ginzton Laboratory, Stanford University, Stanford, CA 94305, USA; jnk1@stanford.edu
[4] Department of Mechanical and Automotive Engineering, Seoul National University of Science and Technology, 232 Gongneung-ro, Nowon-gu, Seoul 01811, Korea
* Correspondence: ikpark@seoultech.ac.kr; Tel.: +82-2-970-6332

Abstract: In this study, TiN thin films fabricated based on the substrate temperature process parameters of a DC magnetron sputtering device and their characteristics are analyzed. TiN thin films are deposited on Si wafer (100) substrates by setting the substrate temperatures to ambient temperature, 100, 200, and 300 °C. The residual stress measurement using the XRD method, adhesion characteristic analysis performed using a nanoscratch test to measure the critical load of the nanoindentation device, and leaky surface acoustic wave (LSAW) measurement were conducted using the V(z) technique of the ultrasonic microscope; the correlations between each measurement were analyzed. The residual stress of the TiN thin film was relieved by up to approximately 48% and adhesion properties enhanced by approximately 10% with an increase in the substrate temperature. In addition, the velocity of the LSAW presented a tendency to increase by up to approximately 5%. The residual stress and velocity of the LSAW were found to be inversely proportional, while the critical load and velocity of the LSAW were directly proportional.

Keywords: acoustic microscopy system (AMS); TiN thin films; micro/nanostructure; V(z) curve; dispersion; surface wave velocity

Citation: Kang, D.; Kim, Y.S.; Kim, J.N.; Park, I.K. Characteristics of TiN Thin Films Deposited by Substrate Temperature Variables Using Scanning Acoustic Microscopy. *Appl. Sci.* **2022**, *12*, 3571. https://doi.org/10.3390/app12073571

Academic Editor: Giuseppe Compagnini

Received: 12 March 2022
Accepted: 29 March 2022
Published: 31 March 2022

1. Introduction

Titanium nitride (TiN) is used in a wide range of applications such as in diffusion barriers in microelectronics, protective coatings on biomedical devices, hard and decorative coatings on machine tools, or in the manufacturing of microgap discharge devices owing to its excellent physical, chemical, electrical, and mechanical properties [1–11]. The physical properties of TiN include high hardness, excellent adhesion properties, wear and corrosion resistance, high melting temperature, thermal and chemical stability, and biocompatibility [11,12]. In the semiconductor industry, TiN is used as a gate electrode and a diffusion barrier layer in complementary metal-oxide semiconductor (CMOS) technology owing to its high electrical conductivity and diffusion barrier properties [13,14]. TiN exhibits very good thermal conductivity and high stability, especially under high-temperature environments, because of its high melting point (2950 °C).

In the TiN thin film deposition process, the adhesion and residual stress characteristics vary depending on the substrate material [15], deposition temperature [9,15], presence of some buffer layer between the substrate [13] and TiN film, and bias voltage of the substrate [9,16]. The production of a TiN thin film by sputtering TiN at a sufficiently high temperature leads to a composition that is similar to that of the stoichiometric bulk material; the substrate temperature during the deposition process has a significant effect on some

properties of the TiN thin film. Thus, an appropriate substrate temperature can improve the adhesion strength of TiN thin films [5–7].

The residual stress and adhesion characteristics of a thin film are critical factors for determining the durability and lifespan of nanostructures. Grazing-incidence X-ray diffraction (GIXD) techniques that use the XRD characteristics [7,8,14,15], etch-back [10], and nanoindenter testing [17] are employed for measuring the residual stress. Further, a nanoscratch test that measures the critical load value at the breakage of a thin film using a nanoindenter [18], the scotch tape test that uses scotch tape [19], and a pull-off test [20] that uses an epoxy coating are employed to measure the adhesion characteristics. These above-mentioned test methods are both destructive and non-destructive characterization techniques; however, they have a limitation in that they require the fracture for measurement.

The application of ultrasound is a promising method for non-destructive residual stress measurement. This method employs the acoustoelastic effect, which is the relationship between the velocity of the ultrasonic wave and the internal/applied stress; further, the method facilitates the understanding about material properties for physical property evaluation, acoustic anisotropy, twin deformation, damaged layer, thin-film thickness measurement, and surface layer residual stress measurement by measuring the speed of sound with high precision in a micro-area. A leaky surface acoustic wave (LSAW) is generated by the V(z) technique; this wave propagates along the surface when the half aperture angle of the acoustic lens of the ultrasonic microscope is greater than the critical angle for generating a surface wave. The LSAW can be used to measure the residual stress and adhesion properties [21–23].

In this study, the characteristics of the deposited TiN thin film are analyzed using the V(z) technique, which measures the velocity of the LSAW propagating along the surface of the material using an ultrasonic microscope as a substrate temperature variable of DC magnetron sputtering. In addition, the correlation between the residual stress measurements performed using a four-fold circled XRD and the adhesion characteristic analysis that uses the scratch test of nanoindentation and the V(z) technique of ultrasonic microscopy is analyzed.

2. Material and Methods

The adhesion characteristics and stress distributions of the thin films were analyzed based on the change in the deposition temperature by using the DC magnetron sputtering method; the deposition conditions are summarized in Table 1. Before the deposition, the Si wafer substrate was cleaned ultrasonically in acetone and an IPA solution for 5 min, respectively, and it was dried by blowing nitrogen gas. The TiN target had a purity of 99.99% and the initial vacuum degree was 3.0×10^{-6} Torr; Ar and N_2 (purity 99.9995%) were used as the working gas, and the flow rate was fixed at 55 sccm. The operating pressure was maintained at 3 mTorr, and the distance from the target to the substrate was set at approximately 7 cm. The DC power was fixed at 6.5 kW, and the substrate temperature was changed to approximately the ambient temperature, 100, 200, and 300 °C, and deposition was performed for approximately 10 min.

Table 1. Process conditions for TiN thin film.

Method	DC-magnetron sputtering
Thin film	TiN thin film
Substrate	4-inch Si wafer
Source gases	Argon gas flow rate: 55 sccm N_2 gas flow rate: 55 sccm
Working pressure	3 mTorr
Substrate temperature (°C)	24, 100, 200, 300

The thickness of the deposited TiN thin film was measured using a scanning electron microscope (UH8010, Hitachi, Tokyo, Japan); the results are shown in Figure 1. TiN thin films (311, 222, 228, and 282 nm) were deposited at the ambient temperature, 100, 200, and 300 °C, respectively.

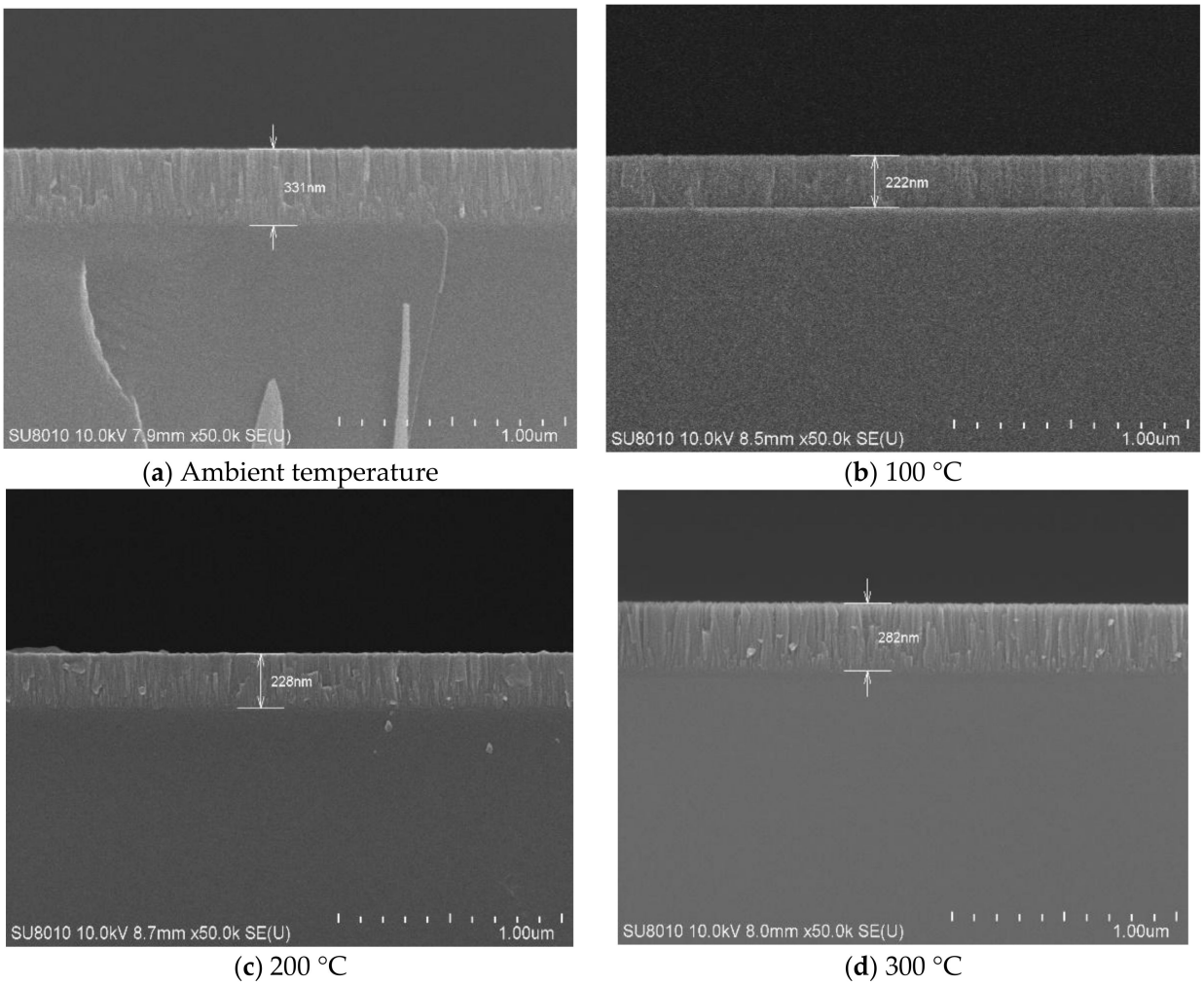

(**a**) Ambient temperature (**b**) 100 °C

(**c**) 200 °C (**d**) 300 °C

Figure 1. SEM cross-sectional image of the TiN thin film deposited with a substrate temperature variation: the thicknesses of the thin films deposited at ambient temperature, 100, 200, and 300 °C are (**a**) 311 nm, (**b**) 222 nm, (**c**) 228 nm, and (**d**) 282 nm, respectively.

The crystal structure was measured using XRD (D/MAX-2500/PC, Rigaku, Tokyo, Japan), and the diffraction pattern, full width half maximum (FWHM) value, grain size, and residual stress of the thin film were also measured to analyze the growth characteristics of the TiN thin film based on the change in substrate temperature. For atomic force microscopy (AFM), surface roughness was measured using an ultrasonic-AFM manufactured in-house in this laboratory; it was measured in the range of 50 × 50 μm. The adhesion properties were measured using the NanoTest for the nanoindenter scratch test. Each correlation was derived by measuring the LSAW using the V(z) curve measurement technique of the ultrasonic microscope Olympus and UH-3 equipment.

3. Results and Discussion

Figure 2 shows the diffraction pattern, FWHM, grain size, and residual stress of the TiN thin film with respect to the change in substrate temperature. The lattice deformation of the TiN thin film was preferentially measured by the 4-fold circle XRD method using the glancing angle XRD. In Figure 2a, the XRD diffraction measured in the range of 2θ = 10° to

100° by scanning at 2°/min shows the diffraction pattern of the TiN thin-film deposited at different substrate temperatures—ambient, 100, 200, and 300 °C. Although several different phases (Ti_3N_2, Ti_4N_3, TiN, Ti_2N) exist, as shown in Figure 2a, peaks in the (111) and (222) directions are observed in the TiN thin film with FCC preferential growth characteristics. In addition, different from other phases in the color of the TiN thin film, the stoichiometry TiN (fcc) surface exhibited a golden color, which is a unique color. This result was consistent with the results of a previous study [24]. The crystal plane of the (111) plane grows according to the change in the substrate temperature, whereas the (222) plane has a relatively low peak intensity and wide FWHM, which indicates that it is a metastable phase close to the amorphous phase. The FWHM value in the main crystal growth direction (111) and grain size were calculated using the Scherer equation to evaluate the FWHM value and grain size of the diffraction peak of the TiN thin film. The Scherer equation is given as [7,13,14].

$$D = \frac{0.9\lambda}{\beta \cos \theta} \quad (1)$$

where λ, β, D, and θ denote the wavelength of the X-ray, value of the half width, grain size, and Bragg angle of the (111) peak, respectively; the calculation results are as shown in Figure 2b.

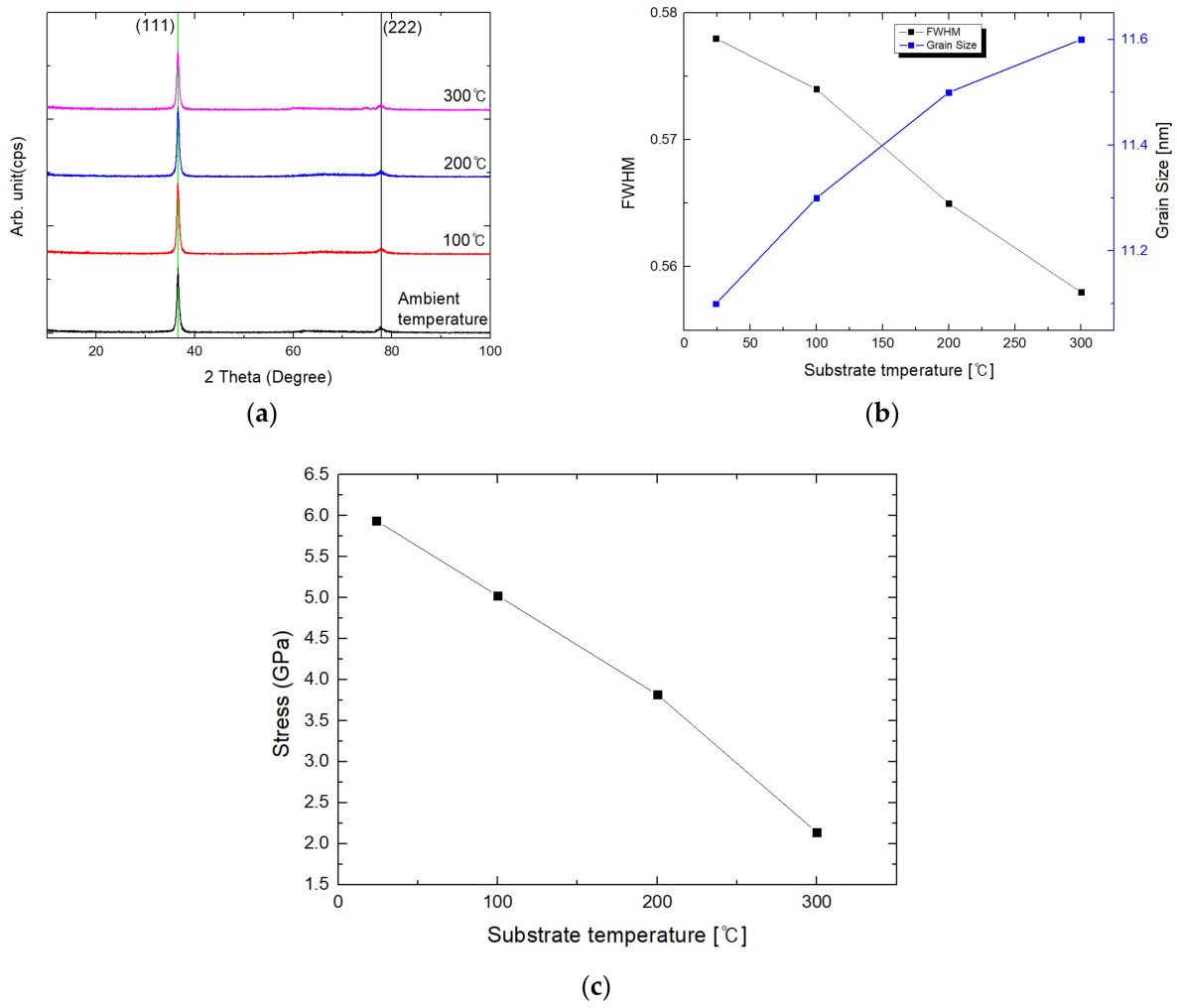

Figure 2. XRD measurement results of the TiN thin film deposition at the varying substrate temperature: (**a**) XRD patterns; (**b**) FWHM and grain size change; (**c**) residual stress change.

The FWHM decreased with an increase in the substrate temperature, and the grain size increased with a decrease in the FWHM value. In terms of the grain size of the TiN thin film, the FWHM in the (111) direction became narrow with an increase in temperature, and the intensity of the peak increased, which increased the grain size. The crystal structure is deformed and the lattice spacing changes in a material with residual stress. That is, the strain rate can be obtained through the change in the interplanar spacing of the crystal lattice; this is formulated as:

$$\epsilon = \frac{d - d_0}{d_0} \quad (2)$$

where d and d_0 represent the spacing between the lattice planes with and without residual stress on the specimen, respectively.

ψ diffraction is performed to rotate the crystal according to the diffraction condition because only the plane parallel to the thin film participates in diffraction; the interplanar distance of the same planes with different crystal directions is obtained by measuring the XRD in a specific 2θ range. The ψ angle and face distance presents a linear relationship by plotting sin2ψ to 2θ(d); the sin2ψ method is used to calculate the residual stress through the slope. The stress can be obtained using Hooke's law by measuring the grid spacing at each location; the residual stress is measured based on the (111) direction and the growth direction of the TiN thin film. The results are shown in Figure 2c.

The residual stress decreased with an increase in the substrate temperature. The synergistic effect of the substrate temperature during TiN thin film deposition is that a metastable phase is generated in the thin film during deposition at ambient temperature, which results in high tensile stress of 5.9 GPa attributed to the deformation of the lattice and occurrence of defects. The high residual stress formed at ambient temperature WAS decreased the defects in the thin film because the substrate temperature increased from 100 to 300 °C owing to the thermal effect applied to the substrate and the decrease in stress caused by the relaxation of the lattice strain.

AFM can be used to measure the quantitative data on the surface roughness of thin films. Figure 3 shows the roughness of the deposited TiN thin film measured according to the substrate temperature variables. The root mean square (RMS) roughness, which is defined as the standard deviation of the surface height profile from the mean height, is the most commonly reported measure of surface roughness; it is calculated as [4].

$$R_{RMS} = \left[\frac{1}{N} \sum_{i=1}^{N} (h_i - < h >)^2 \right]^{1/2} \quad (3)$$

where N, h_i, and h_i denote the number of pixels in the image, the height of the i-th pixel, and the average height of the image, respectively. Thus, information about the vertical direction of the thin film can be obtained.

Figure 3 shows the RMS values of the TiN thin films. Figure 3a–d shows images according to the substrate temperatures; the RMS roughness values were measured at 0.90, 0.93, 1.07, and 1.24 nm at ambient temperature, 100, 200, and 300 °C, respectively. The results and trends are shown in Figure 3e. The RMS roughness value of the TiN thin film increased with an increase in the substrate temperature.

A nanoscratch test was conducted using the NanoTest (NTX, Micro Materials, Wrexham, UK). In the nanoscratch test, the load at the point where the thin film falls from the substrate is called the critical load, and the work of adhesion is calculated through this load. The work of adhesion is expressed based on the relationship between the compressive and shear stresses through the energy balance theory as [17].

$$W_{AD} = \frac{\sigma^2 t}{2E} + \frac{\gamma^2 t}{2G} \quad (4)$$

where W_{AD}, σ, t, E, γ, and G denote the work of adhesion, compressive stress, thickness of the thin film, elastic modulus, shear stress, and shear modulus, respectively. In the actual

scratch test, the second term in Equation (4) can be neglected because the shear stress that occurs when the thin film falls is very small compared to the compressive stress. Thus, Equation (4) can be rearranged as:

$$\sigma = \left(\frac{2EW_{AD}}{t}\right)^{1/2} \tag{5}$$

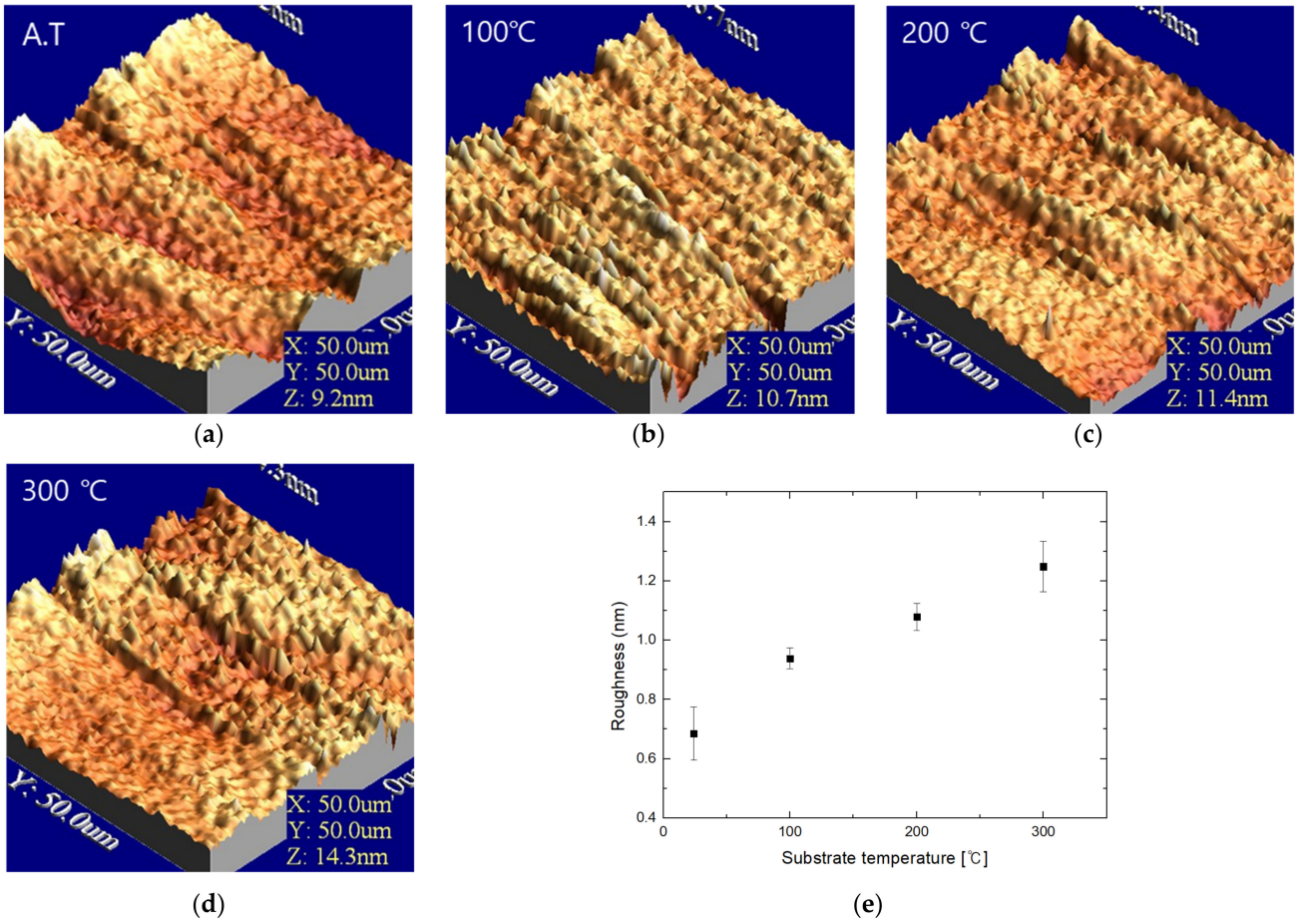

Figure 3. AFM image of thin films with different substrate temperatures: (**a**) ambient temperature (~24 °C); (**b**) 100 °C; (**c**) 200 °C; (**d**) 300 °C; and (**e**) RMS roughness.

In the equation $\sigma = F/A$ between the stress and the load, F is expressed as the critical load (L_C) under which the thin film falls from the substrate and cross-sectional area A is assumed to be half of the projected area of the indenter; this is expressed as:

$$\sigma = \frac{8L_c}{\pi d^2} \tag{6}$$

where d denotes the width of the scratch. Equations (5) and (6) can be rearranged for the critical load at which the thin film fracture occurs, and this can be expressed as

$$L_C = \frac{\pi d^2}{8}\left(\frac{2EW_{AD}}{t}\right)^{1/2} \tag{7}$$

Since the thickness and elasticity of the thin film are set to the same value in the experiment to be performed, Equation (7) implies a proportional relationship between L_C and W_{AD}. In this study, L_C measured by the nanoscratch measurement is assumed to be the adhesion force because the experiment was conducted on specimens composed of the same

material. The indenter used for measurement was a cone-shaped diamond tip. Considering the hard coating, the scratch length was set to 300 µm. The measurement started with an initial load of 0.01 mN, and the force was increased at a rate of 1.5 mN/s until the final load set to 150 mN. The detailed settings for the scratch test are presented in Table 2.

Table 2. Experimental setup of the nanoscratch test.

Tip type	5 µm sphero-conical
Initial load (mN)	0.01
Final load (mN)	150
Loading rate(mN/s)	1.5
Speed (µm/s)	2
Length (µm)	300

Figure 4 shows the results of the nanoscratch test on the deposited thin film test piece according to the substrate temperature process parameters of the TiN thin film. The scratch test was performed 10 times for each test piece to verify the error and reliability. The exact load at the desired location can be calculated based on the known fracture point because the load constantly increases according to the scratch length. Figure 4 shows the scratch results for each specimen. The nanoscratch test results revealed that the overall adhesion strength increased with an increase in the substrate temperature. A denser thin film structure was formed on the substrate surface because of the increase in the mobility of atoms at the temperature of the substrate during thin film deposition, which contributed to the improvement in the adhesion properties.

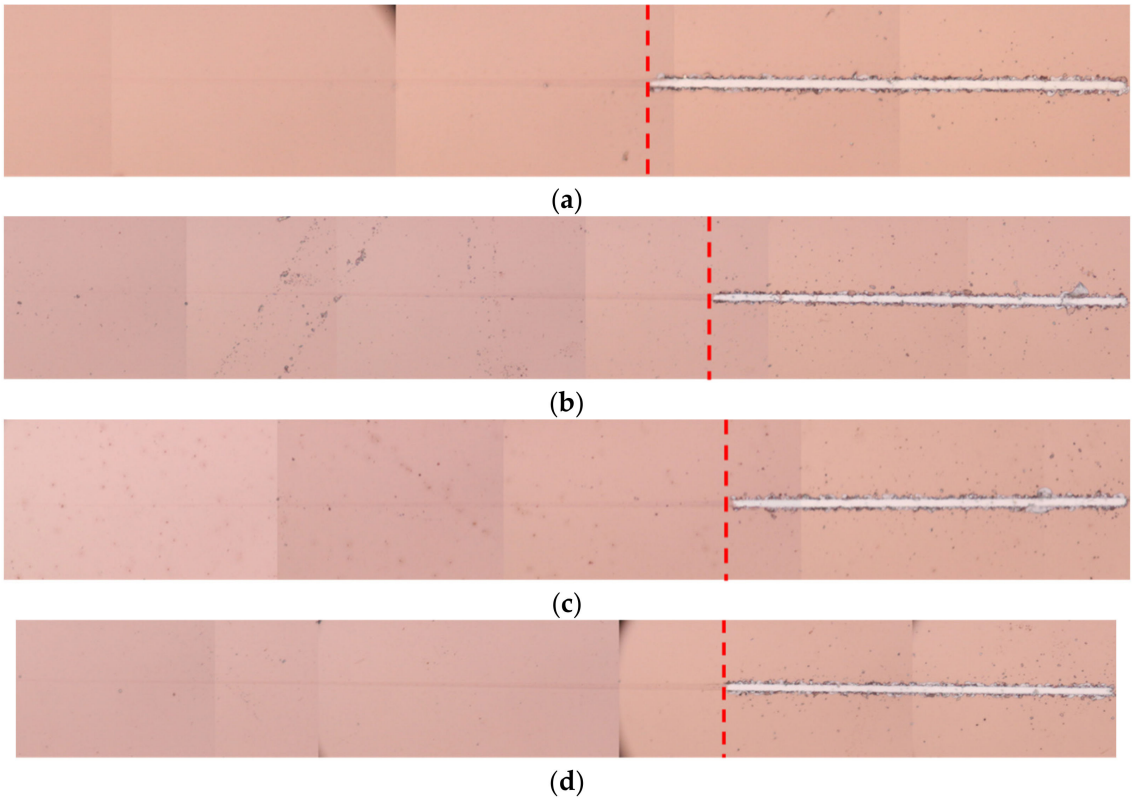

(**a**)

(**b**)

(**c**)

(**d**)

Figure 4. *Cont.*

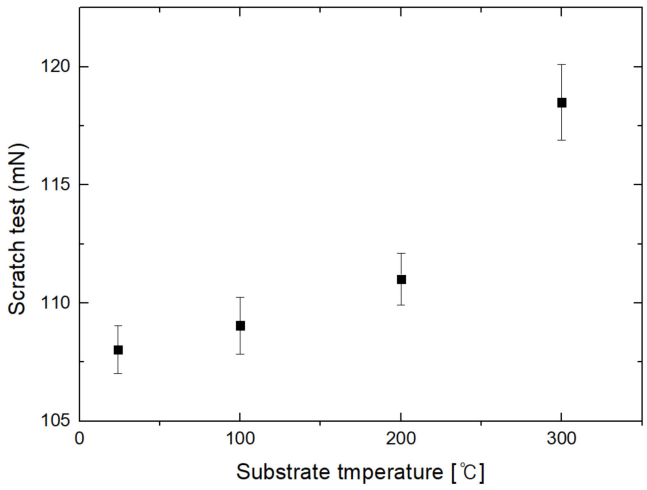

(**e**)

Figure 4. OM image of the nanoscratch test: (**a**) ambient temperature (~24 °C); (**b**) 100 °C; (**c**) 200 °C; (**d**) 300 °C; and (**e**) critical adhesive strengths at each temperature using the nanoscratch test are 108.03, 109.05, 111.02, and 118.5 mN, respectively.

The phase velocity of the LSAW was measured using V(z) technique scanning acoustic microscopy to evaluate the adhesion interface characteristics of the prepared specimen. The velocity of the surface wave was measured using the V(z) technique of ultrasonic microscopy. The V(z) technique calculates the velocity of a surface wave by superimposing a signal incident or reflected vertically from the focusing probe lens and a leakage signal of the surface wave incident along with the shape of the lens at an angle greater than or equal to the second critical angle and propagated along the surface of the specimen. The waveform of the signal according to the defocused distance (z) of the probe lens is called the V(z) curve; the distance between the signal peaks is called the value of Δz. The velocity of the surface wave is defined as [21].

$$C_{SAW} = 1 - \left[\left(1 - \frac{C_W}{2f\Delta z}\right)^z\right]^{-1/2} \quad (8)$$

where C_W denotes the longitudinal wave velocity of the contact medium, and f denotes the applied frequency.

UH-3 (Olympus Corp.) was used as a piece of scanning acoustic microscope equipment for measuring the V(z) technique. A 400 MHz transducer in the high-frequency band was selected and measured to evaluate the characteristics of the nanoscale thin film more clearly. Detailed experimental conditions were set as summarized in Table 3. The velocity of the LSAW was measured using the V(z) technique, and the results are shown in Figure 5.

Table 3. Experimental conditions for the leaky surface acoustic wave.

Apparatus	UH-3 (Olympus Corp.)
Acoustic lens	Model: AL4M631
Frequency	400 MHz
Working distance	310 μm
Apparatus angle	120° (second critical angle)
Couplant	De-ionized water (21.5 °C)

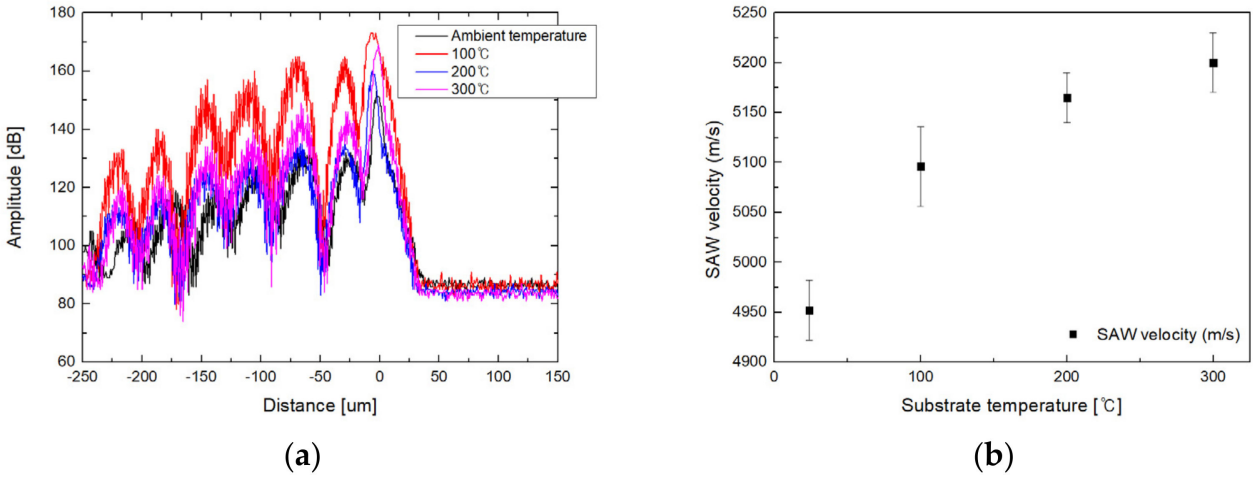

Figure 5. Measurement of V(z) curve using scanning acoustic microscopy of TiN thin film deposited as a variable of substrate temperature: (**a**) measured V(z) curve; (**b**) change in the surface acoustic wave velocity corresponding with the substrate temperature variable.

Figure 5a shows the V(z) curve of the TiN thin film deposited as a substrate temperature variable. Figure 5b shows this V(z) curve expressed through fast Fourier transform analysis. The average was calculated by measuring the TiN thin film deposited with each substrate temperature variable 10 times; this value was approximately 4952, 5092, 5165, and 5200 m/s for the deposition at ambient temperature, 100, 200, and 300 °C, respectively. The velocity of the ultrasonic longitudinal wave tended to increase with an increase in the temperature of the substrate during deposition. The barrier to the propagation of leaky surface waves was reduced because of the reduction in the defects in the microstructure inside the TiN thin film and the reduction in grain boundaries caused by the growth of grains, which increased the velocity of the LSAW.

Table 4 shows the overall results of XRD stress, nanoindentor scratch test, AFM roughness, and SAM V(z) curve. In this study, the residual stress and bonding characteristics of the deposited TiN thin film were measured at DC magnetron sputtering substrate temperature variables, and the correlation with the leakage surface acoustic wave velocity was comparatively analyzed through the measurement of the V(z) curve of SAM. As a result, LSAW velocity, nanoscratch test, RMS roughness values, and residual stress values were measured to be inversely proportional. The residual stress and velocity of the surface acoustic wave are inversely proportional, and the change in the critical load value, surface roughness, and velocity of the surface acoustic wave are proportional.

Table 4. Overall results of the TiN thin film measurement experiment.

	LSAW Velocity (m/s)	Residual Stress (Gpa)	Nanoscratch Test (mN)	RMS Roughness (nm)
Ambient temperature	4952	5.938	108.03	0.685
100 °C	5096	5.024	109.05	0.938
200 °C	5165	3.818	111.02	1.078
300 °C	5200	2.138	118.05	1.248

4. Conclusions

The surface and mechanical properties of a TiN thin film deposited as the substrate temperature process variable of the DC magnetron sputtering system were studied using different techniques including both destructive and non-destructive methods. The TiN thin film showed a 48% relaxation of the residual stress from about 5.9 GPa at ambient

temperature to about 2.138 GPa at 300 °C; this was attributed to the reduction in the defects and the relaxation of the lattice strain in the thin film caused by the effect of the heat applied to the substrate.

The adhesion properties were approximately 108.03, 109.05, 111.02, and 118.05 mN at ambient temperature, 100, 200, and 300 °C, respectively. The adhesion of the TiN thin film was improved as the substrate temperature increased.

The changes in the surface wave velocity of the LSAW observed using the ultrasonic microscope of the TiN thin film were approximately 4952, 5096, 5165, and 5200 m/s at ambient temperature, 100, 200, and 300 °C, respectively. The surface wave velocity of the TiN thin film deposited at 300 °C was about 5% higher than that of the TiN thin film deposited at ambient temperature. The presented data suggest that the adhesion properties of the TiN thin film tended to increase with a decrease in the residual stress; the velocity of the LSAW also tended to increase. The residual stress and velocity of the surface acoustic wave are inversely proportional, and the change in the critical load value and the velocity of the surface acoustic wave are proportional.

These results can be applied to the evaluation of the residual stress and adhesion properties of thin films using the V(z) technique using an ultrasonic microscope.

Author Contributions: Conceptualization, D.K. and Y.S.K.; methodology, D.K.; validation, D.K., Y.S.K., J.N.K. and I.K.P.; formal analysis, D.K. and Y.S.K.; investigation, D.K.; data curation, D.K.; writing—original draft preparation, D.K.; writing—review and editing, D.K., Y.S.K., J.N.K. and I.K.P.; visualization, D.K. and Y.S.K.; supervision, I.K.P.; project administration, D.K.; funding acquisition, I.K.P. All authors have read and agreed to the published version of the manuscript.

Funding: This study was supported by the Research Program funded by the Seoul Tech (Seoul National University of Science and Technology), grant number 2021-1168.

Institutional Review Board Statement: Not applicable.

Informed Consent Statement: Not applicable.

Data Availability Statement: Not applicable.

Conflicts of Interest: The authors declare no conflict of interest.

References

1. Vasu, K.; Krishna, M.G.; Padmanabhan, K. Substrate-temperature dependent structure and composition variations in RF magnetron sputtered titanium nitride thin films. *Appl. Surf. Sci.* **2011**, *257*, 3069–3074. [CrossRef]
2. Vaz, F.; Ferreira, J.; Ribeiro, E.; Rebouta, L.; Lanceros-Méndez, S.; Mendes, J.; Alves, E.; Goudeau, P.; Rivière, J.; Moutinho, I.; et al. Influence of nitrogen content on the structural, mechanical and electrical properties of TiN thin films. *Surf. Coat. Technol.* **2005**, *191*, 317–323. [CrossRef]
3. Holmberg, K.; Ronkainen, H.; Laukkanen, A.; Wallin, K.; Hogmark, S.; Jacobson, S.; Wiklund, U.; Souza, R.M.; Ståhle, P. Residual stresses in TiN, DLC and MoS2 coated surfaces with regard to their tribological fracture behaviour. *Wear* **2009**, *267*, 2142–2156. [CrossRef]
4. Gelali, A.; Ahmadpourian, A.; Bavadi, R.; Hantehzadeh, M.R.; Ahmadpourian, A. Characterization of Microroughness Parameters in Titanium Nitride Thin Films Grown by DC Magnetron Sputtering. *J. Fusion Energy* **2012**, *31*, 586–590. [CrossRef]
5. Ghobadi, N.; Ganji, M.; Luna, C.; Arman, A.; Ahmadpourian, A. Effects of substrate temperature on the properties of sputtered TiN thin films. *J. Mater. Sci. Mater. Electron.* **2015**, *27*, 2800–2808. [CrossRef]
6. Durusoy, H.Z.; Duyar, Ö.; Aydınlı, A.; Ay, F. Influence of substrate temperature and bias voltage on the optical transmittance of TiN films. *Vacuum* **2003**, *70*, 21–28. [CrossRef]
7. Bavadi, R.; Valedbagi, S. Physical properties of titanium nitride thin film prepared by DC magnetron sputtering. *Mater. Phys. Mech.* **2012**, *15*, 167–172.
8. Wang, A.-N.; Huang, J.-H.; Hsiao, H.-W.; Yu, G.-P.; Chen, H. Residual stress measurement on TiN thin films by combing nanoindentation and average X-ray strain (AXS) method. *Surf. Coat. Technol.* **2015**, *280*, 43–49. [CrossRef]
9. Patsalas, P.; Charitidis, C.; Logothetidis, S. The effect of substrate temperature and biasing on the mechanical properties and structure of sputtered titanium nitride thin films. *Surf. Coat. Technol.* **2000**, *125*, 335–340. [CrossRef]
10. Machunze, R.; Janssen, G. Stress gradients in titanium nitride thin films. *Surf. Coat. Technol.* **2008**, *203*, 550–553. [CrossRef]
11. Liu, J.-n.; Xu, B.-s.; Wang, H.-d.; Cui, X.-f.; Jin, G.; Xing, Z.-g. Effects of Loading Frequency and Film Thickness on the Me-chanical Behavior of Nanoscale TiN Film. *J. Mater. Eng. Perform.* **2017**, *26*, 4381–4390. [CrossRef]

12. Yang, Z.; Lee, Y. Effect of the welding residual stress redistribution on impact absorption energy. *J. Weld. Join.* **2015**, *33*, 72–79. [CrossRef]
13. Subramanian, B.; Ashok, K.; Jayachandran, M. Effect of substrate temperature on the structural properties of magnetron sputtered titanium nitride thin films with brush plated nickel interlayer on mild steel. *Appl. Surf. Sci.* **2008**, *255*, 2133–2138. [CrossRef]
14. Xi, Y.; Gao, K.; Pang, X.; Yang, H.; Xiong, X.; Li, H.; Volinsky, A. Film thickness effect on texture and residual stress sign transition in sputtered TiN thin films. *Ceram. Int.* **2017**, *43*, 11992–11997. [CrossRef]
15. Gómez, A.; Recco, A.; Lima, N.; Martinez, L.; Tschiptschin, A.; Souza, R. Residual stresses in titanium nitride thin films obtained with step variation of substrate bias voltage during deposition. *Surf. Coat. Technol.* **2010**, *204*, 3228–3233. [CrossRef]
16. Benegra, M.; Lamas, D.; de Rapp, M.F.; Mingolo, N.; Kunrath, A.; Souza, R. Residual stresses in titanium nitride thin films deposited by direct current and pulsed direct current unbalanced magnetron sputtering. *Thin Solid Films* **2005**, *494*, 146–150. [CrossRef]
17. Schoeppner, R.; Ferguson, C.; Pethö, L.; Guerra-Nuñez, C.; Taylor, A.A.; Polyakov, M.; Putz, B.; Breguet, J.-M.; Utke, I.; Michler, J. Interfacial adhesion of alumina thin films over the full compositional range of ternary fcc alloy films: A combinatorial nanoindentation study. *Mater. Des.* **2020**, *193*, 108802. [CrossRef]
18. Vardaki, M.; Pantazi, A.; Demetrescu, I.; Enachescu, M. Assessing the Functional Properties of TiZr Nanotubular Structures for Biomedical Applications, through Nano-Scratch Tests and Adhesion Force Maps. *Molecules* **2021**, *26*, 900. [CrossRef]
19. Seok, S.; Park, H.; Kim, J. Characterization and Analysis of Metal Adhesion to Parylene Polymer Substrate Using Scotch Tape Test for Peripheral Neural Probe. *Micromachines* **2020**, *11*, 605. [CrossRef] [PubMed]
20. Acda, M.; Devera, E.E.; Cabangon, R.J.; Ramos, H.J. Effects of plasma modification on adhesion properties of wood. *Int. J. Adhes. Adhes.* **2012**, *32*, 70–75. [CrossRef]
21. Park, T.-S.; Choi, Y.-M.; Cho, B.-S.; Park, I.-K. Analysis of Dispersion Characteristics of Rayleigh Waves in Nanostructured Thin Films. *J. Korean Soc. Nondestruct. Test.* **2018**, *38*, 98–106. [CrossRef]
22. Ohashi, Y.; Arakawa, M.; Kushibiki, J.-i. Improvement of Velocity Measurement Accuracy of Leaky Surface Acoustic Waves for Materials with Highly Attenuated Waveform of the V(z) curve by the Line-Focus-Beam Ultrasonic Material Characterization System. *Jpn. J. Appl. Phys.* **2006**, *45*, 4505–4510. [CrossRef]
23. Kim, H.J.; Lee, M.Y.; Bin Jeong, H.; Park, I.G.; Cho, I.S. Residual Stress Measurement Method Using Ultrasonic Acoustic Velocity. *Trans. KSME C Ind. Technol. Innov.* **2019**, *7*, 33–40. [CrossRef]
24. Kumar, N.; Fissel, M.; Pourrezaei, K.; Lee, B.; Douglas, E. Growth and properties of TiN and TiOxNy diffusion barriers in silicon on sapphire integrated circuits. *Thin Solid Films* **1987**, *153*, 287–301. [CrossRef]